Available online at www.sciencedirect.com
SCIENCE DIRECT®
Biomaterials 25 (2004) 4195–4201
Biomaterials
www.elsevier.com/locate/biomaterials

Biocompatibility of sorbitol-containing polyesters. Part I: Synthesis, surface analysis and cell response in vitro ☆

Ying Mei[a], Ajay Kumar[a], Wei Gao[a], Richard Gross[a,*], Scott B. Kennedy[b], Newell R. Washburn[b], Eric J. Amis[b], John T. Elliott[c]

[a] *Department of Chemistry and Chemical Engineering, NSF-I/UCRC Center for Biocatalysis and Bioprocessing of Macromolecules, Polytechnic University, Six Metrotech Center, Brooklyn, NY 11201, USA*
[b] *Polymers Division, National Institute of Standard and Technology, 100 Bureau Drive, Stop 8540, Gaithersburg, MD 20899-8540, USA*
[c] *Biotechnology Division, National Institute of Standard and Technology, 100 Bureau Drive, Stop 3460, Gaithersburg, MD 20899-3460, USA*

Received 27 January 2003; accepted 10 October 2003

Abstract

A series of sorbitol-containing polyesters were synthesized via a one-pot lipase-catalyzed condensation polymerization. Thin films were prepared by spin coating on silicon wafers and surfaces were analyzed by tapping mode atomic force microscopy and contact angle measurements. Surface morphologies and surface energies across the series of polyester films, including a poly(ε-caprolactone) (PCL) control were nearly indistinguishable. Biocompatibility of the sorbitol-containing polyester series was evaluated against a PCL control by measuring cell spreading and proliferation of a mouse fibroblast 3T3 cell line in vitro. Results confirmed that the sorbitol-containing polyester surfaces elicited cell behavior similar to the PCL control. These results establish the sorbitol-containing polyester series as a promising material for tissue engineering research and development.

Keywords: Functional polymer; Biocompatibility; Fibroblast; Population distribution

1. Introduction

Tissue engineering has received much attention in recent years because it promises a method to repair or regenerate damaged tissues and organs. This is evidenced both in academia and industry by the escalating number of publications and increased resource investment [1,2]. It is expected that the next generation of biomaterials will exhibit biodegradability, biocompatibility, and the ability to stimulate specific cellular response at the molecular level [3,4].

Polyesters such as poly(lactic acid) and poly(ε-caprolactone) (PCL) are used as biomaterials because they demonstrate both biodegradability and biocompatibility. However, the lack of tissue integration and specific bioactivity remains problematic for developing more advanced biomaterials [5,6]. As such, incorporation of various functional groups into polyester matrices has been investigated for the purpose of attaching biological molecules such as oligopeptides or oligosaccharides. While these investigations are informative, the preparation of functional polyesters usually involves tedious protection/deprotection chemistry and the use of organic solvents [7,8]. As a result, such systems present significant challenges for transferring technology from the lab to development.

Lipase-catalyzed polymerizations have attracted much attention in recent years because they can provide high efficiency, good enantio- and regio-selectivity, proceed in the absence of solvents, and circumvent potentially toxic catalysts [9,10]. Previously, we reported a one-pot synthesis of novel sugar-containing polyesters benefiting from lipase regioselectivity [11]. Sugar segments along the backbone provide functional groups for further modification without the use of tedious protection/deprotection chemistry and organic solvents. We begin the process of investigating these materials by establishing the baseline characteristics of unmodified,

☆ Certain equipment and instruments or materials are identified in the paper to adequately specify the experimental details. Such identification does not imply recommendation by the National Institute of Standards and Technology, nor does it imply the materials are necessarily the best available for the purpose.

*Corresponding author.

0142-9612/$ - see front matter © 2003 Elsevier Ltd. All rights reserved.
doi:10.1016/j.biomaterials.2003.10.087

sugar-containing polyesters. Surface properties are characterized by atomic force microscopy (AFM) and contact angle measurements, and biocompatibility is assessed by measuring cell morphology, spreading and cell proliferation of mouse fibroblast 3T3 in vitro.

2. Materials and methods

2.1. Polyester preparation and characterizations

Novozyme-435 beads were supplied by Novozyme (Denmark). All other chemicals were purchased from Aldrich and used as received. ^{1}H NMR spectra were recorded on a Bruker NMR spectrometer (model DPX 300) at 300 MHz. The chemical shifts in parts per million (ppm) for ^{1}H NMR spectra were referenced relative to tetramethylsilane (TMS, 0.00 ppm) as the internal reference. Polymer was characterized by a gel permeation chromatography- multiangle light scattering (GPC-MALS) system consisting of a waters 510 pump, a 717 plus auto-injector, a Wyatt DAWN DSP multi-angle laser light scattering photometer (Wyatt Technology, Santa Barbara, CA), and an Optilab DSP refractometer (Wyatt Technology). A three-column set consisting of $300 \times 7.8\,mm^2$ Styragel HR4, HR3 and HR1 was used to chromatograph the samples at room temperature. Chloroform was used as the mobile phase at a flow rate of 1 ml/min. Absolute molecular weights were determined using the ASTRA light scattering software (Wyatt Technology).

The preparation of poly(apidic acid-co-octanediol-co-sorbitol) (PAOS) was previously described in Ref. [11]. Briefly, in a typical reaction, apidic acid (2.92 g, 0.02 mol), octanediol (2.63 g, 0.018 mol) and sorbitol (0.365 g, 0.002 mol) were mixed at 120°C in a 25 ml round bottom flask with a stir bar. After thorough mixing of all reaction components, the reaction temperature was decreased slowly to 95°C, and Novozyme-435 (0.59 g) was added to the reaction. The temperature was lowered and held at 90°C for 2 h at which point vacuum (13.33 Pa) was applied. The polymerization proceeded at 90°C under vacuum for 48 h. The crude product was dissolved in chloroform, precipitated in cold methanol, vacuum dried at room temperature for 12 h, and 4.1 g of the sorbitol-containing polyester was obtained.

2.2. Polymer film preparation

Silicon wafers were washed with a soap solution, rinsed with deionized water and blown dry with nitrogen. After this initial cleaning, wafers were cut to ca. 1cm × 1 cm and exposed to UV/ozone for 1 min. The silicon substrates were then rinsed with toluene and immersed in a solution of octyldimethylchlorosilane in toluene (mass fraction of 1.5%) at room temperature. After 1 h, substrates were rinsed with toluene and dried at 120°C under vacuum for 1 h. The polymer films were spin coated from a chloroform solution (mass fraction of 2%) at 165 rad/s and the films were dried at room temperature under vacuum for 24 h.

2.3. AFM analysis

Surface morphology of the polymer film was visualized using an AFM Digimension 3100, (Digital Instruments) in air at room temperature. The surface was continuously imaged under tapping mode with a scanned area of $20 \times 20\,\mu m^2$ and a scan speed of 1 Hz. The surface roughness was assessed by the root mean square (RMS) average of height deviations taken from the mean data plane, and the arithmetic average of the absolute values of the height deviations taken from the mean data plane (R_a).

2.4. Contact angle measurement

Contact angle measurements were performed at room temperature with a Kruss *G*2 contact angle measuring system using water as the probe fluid. Advancing contact angles were recorded while the probe fluid was added to the drop. Static contact angles were recorded within 1 min of depositing a drop on the surface. The standard uncertainty of contact angle measurements was determined by the standard deviation between six independent measurements per sample.

2.5. Cell culture

Mouse fibroblast 3T3 cells were a gift from Dr. Kenneth Yamada at NIH. The cells were cultured using Dulbecco's modified Eagle's medium (DMEM) supplemented with calf serum (volume fraction of 10%) and penicillin/streptomycin (volume fraction of 1%). All solutions were obtained from Gibco, UK. Cells were incubated at 37°C under 10% CO_2. Cells grown to preconfluence were passaged by trypsinization for 1 min twice at 37°C, diluted, and inoculated into a fresh tissue culture flask.

Fibroblasts were seeded at a density of 10,000 cells/well (2200 cells/cm^2) in a 12-well plate onto polymer films. After incubating for 24 h, the cells were washed with phosphate buffered saline (PBS) and fixed with glutaraldehyde (Sigma) in PBS (volume fraction of 1.5%) for 1 h at room temperature. Cells were then rinsed with a Triton X-100, PBS solution (volume fraction of 0.1%) for 5 min to permeabilize cell membranes and stained with 0.02% by mass Texas Red-C_2 maleimide (molecular probes) in 50/50 (v/v) glycerol/PBS solution. Samples were rinsed with a PBS solution and mounted using vector shield containing the

4,6-diamidino-2-phenylindole (DAPI) nuclear counterstain.

2.6. Fluorescence microscopy and cell image analysis

Images were taken using an inverted microscope equipped with a fluorescence filter. About 50 image sets were collected at random positions from each sample. An image set consisted of one image of the Texas Red fluorescence and a corresponding image of the DAPI fluorescence. Each material was run in triplicate, producing about 150 image sets for one material surface covering an area of approximate 90 mm^2. Automated image analysis was performed by detecting variations in image color intensity and calculating individual cell parameters based on the fluorescence signal per pixel [12].

The automated analysis generated a data spreadsheet containing a variety of measured parameters including object area, roundness, aspect ratio and perimeter. Two columns from this spreadsheet were chosen for further analysis: object areas (from the Texas Red fluorescence) corresponding to the area of a cell or group of overlapping cells, and the number of nuclei (from the DAPI fluorescence) within each object. Cell density for a given material is reported as the total area of all frames analyzed divided by the total number of cell nuclei. Cell spreading is reported by sorting the two column data and removing all objects containing zero nuclei (dust, debris, etc.), all objects containing two or more nuclei (overlapping cells), and the largest 1% of the remaining population (most, but not all "giant" cells). Overlapping cells are not included because this study seeks to investigate cell–biomaterial interactions independent of cell–cell interactions.

After sorting and deleting the indicated objects, distributions were smoothed using a nonparametric kernel density estimator [13]. This process facilitates visual comparison of the distributions without forcing parametric fits that may or may not accurately depict the true distribution. Quantitative distribution comparisons were performed by a nonparametric, two-sample Kolmogorov–Smirnov (K–S) test [13].

3. Results and discussion

3.1. Synthesis and characterization of the polyester

The purpose of this study was to prepare and evaluate a promising new class of biomaterials, sugar-containing polyesters. Sorbitol was chosen as a functional comonomer in this study because it has a low melting point that facilitates the polymerization in bulk. Furthermore, the unreacted pendant hydroxyl groups make these promising candidates for further chemical modification. Fig. 1 illustrates the chemical structure of the polyester series reported herein. Table 1 lists the feed monomer ratios along with the corresponding product compositions and molecular weights. The compositions and absolute molecular weights reported in Table 1 were determined by ^{1}H NMR and GPC-MALS, respectively. Poly(apidic acid-co-octanediol-co-sorbitol) (PAOS) containing 1%, 5%, 12% and 18% mol fraction sorbitol units have relative molar mass values that are similar (43,000–60,000). However, the 27% mol fraction copolymer has a relative molar mass value of 117,000. We believe that the high molecular weight reported for 27% PAOS is due to branching and an increased propensity

Table 1
Monomer feed ratios (mol to mol), polymer compositions (mol to mol), and molecular weights of sorbitol containing polyesters

Feed ratio (S:O:A)	Composition ratio (S:O:A)	Absolute Mw ($\times 10^{-3}$)	Polydispersity (Mw/Mn)
1:99:100	1:99:100	60	2.60
5:95:100	5:95:100	43	2.10
10:90:100	12:88:100	44.2	2.26
20:80:100	18:82:100	47.6	2.27
30:70:100	27:63:100	117	3.40

S: sorbitol, O: octanediol, A: adipic acid.

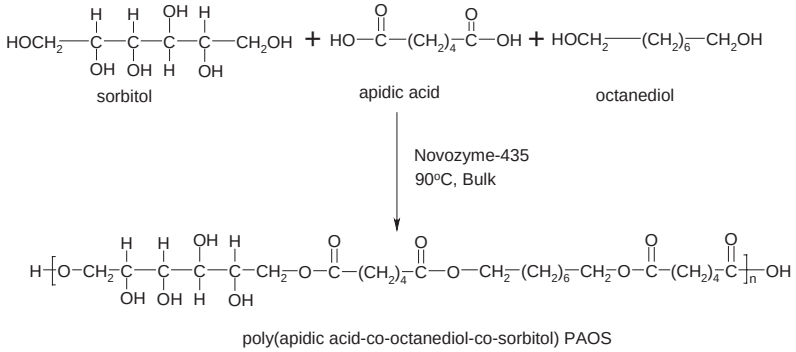

Fig. 1. Preparation of PAOS.

for interchain coupling reactions that occur between nonchain end repeat units.

3.2. Characterization of polyester surface

Recent investigations of cell behavior on thin polymer films have shown that surface roughness and surface energy play an influential role in eliciting cell behavior. To study the effect of sorbitol content in the polyester on the surface morphology, the surface morphology of the PAOS were studied by tapping mode AFM. Fig. 2 shows the AFM height images of the top surfaces of the polymer films in a two-dimensional form over an area of $20 \times 20\,\mu m^2$. Polygonal spherulite structures are seen in all samples to varying degrees. When the sorbitol content reaches 18% by mol fraction the polygon boundary is no longer fully clear. When the sorbitol content is 27% by mol fraction, the boundary is difficult to find. This observation indicates that increased sorbitol content inhibits the formation of the spherulite structure because the sorbitol units do not fit within the poly(octanyladipate) crystalline lattice. The disruption of the spherulite structure may be further exacerbated by the rigidity of sorbitol and the hydrogen bonding between sorbitol segments. Indeed, X-ray diffraction analysis by comparing crystalline phase peak area to crystalline and noncrystalline phase area showed that with an increase in the sorbitol content from 0% to 27% mol fraction the crystallinity decreased from 64% to 47% [14].

Differences in surface morphology are quantified by measuring RMS and R_a and the results are reported in Fig. 3. The error bars in Figs. 3 and 7 represent the standard uncertainty based on one standard deviation of the data measured. RMS is the root mean square average of height deviations taken from the mean data plane, and R_a is the arithmetic average of the absolute values of the height deviations taken from the mean data plane. Notice that the RMS monotonically decreases from 16 to 8 nm as the sorbitol content of the PAOS increases from 1% to 27% mol fraction. R_a follows the same trend as RMS. These measurements are consistent with the hypothesis that the presence of sorbitol units along the polymer backbone disrupts crystalline ordering.

In addition to altering crystallinity, the presence of sorbitol in the polymer backbone could also affect surface energy. Contact angle measurements are widely used as a simple, sensitive technique for quantifying the hydrophilic/hydrophobic property of a surface. Therefore, aqueous static and dynamic contact angle measurements were carried out to investigate whether the presence of sorbitol would cause the water contact angle

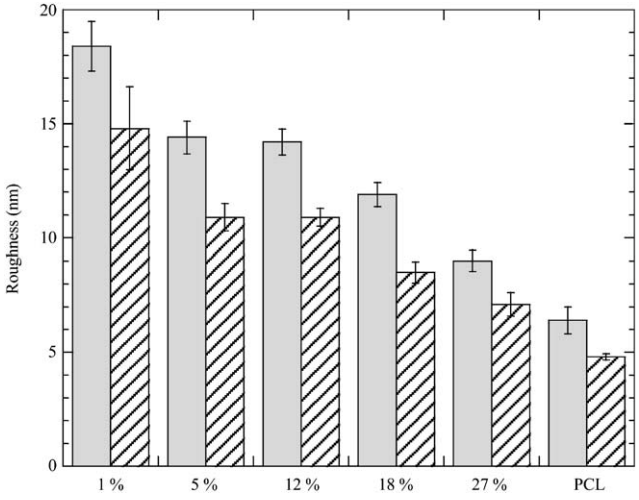

Fig. 3. RMS (shaded) and R_a (single hatch) values of PAOS and PCL films. Percentages represent the mole fraction of sorbitol.

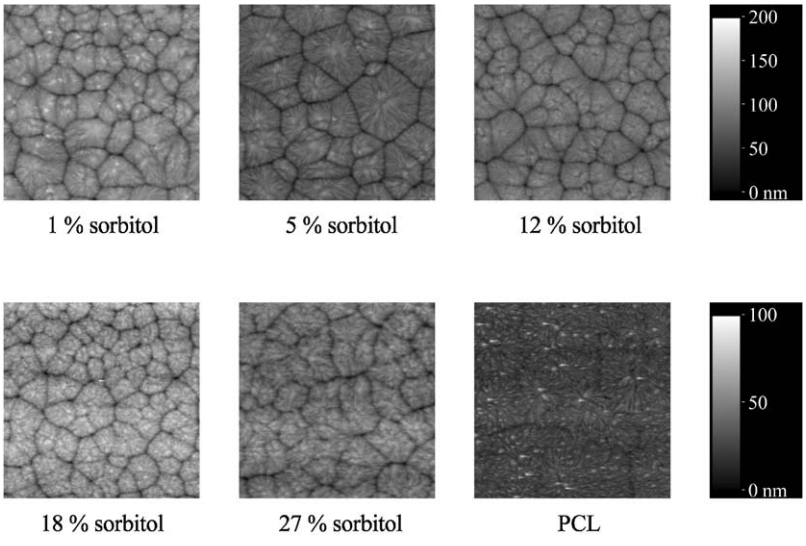

Fig. 2. AFM images of the top surfaces of PAOS polymers and PCL. Percentages represent the mole fraction of sorbitol. All images are $20 \times 20\,\mu m^2$.

to decrease. While measurable differences were observed between samples, all were hydrophobic with contact angles between 80° and 90°. Furthermore, the differences did not follow a discernable trend with respect to sorbitol content and all samples maintained their hydrophobic character, even after soaking in water for 24 h. This indicates that, in air, the hydrophobic segments made from apidic acid and octanediol are oriented towards the surface to minimize the surface energy and stabilize the polymer–air interface. This inability of the surface to rearrange and respond to the water droplet by altering the contact angle occurs irrespective of the fact that these copolymers have T_g values well below room temperature ($\approx -15°C$) [11]. It may be that the crystallization process during solvent evaporation at room temperature occurs so that most of the hydrophilic sorbitol segments are isolated within crystalline phases or are restricted by hydrogen bonding between inter/intra polyester chains. In any case, sorbitol units appear to be restricted from reorienting to the surface when it is wetted.

In this study, PCL was chosen as a control because it is an FDA approved biodegradable and biocompatible polymer and PCL has a similar chemical structure with the PAOS. Unsurprisingly, the PCL appears to have a similar surface morphology and hydrophobicity as the PAOS copolymers.

3.3. Cell spreading and proliferation

The NIH 3T3 fibroblast cell line was chosen for this study because it provides a robust and durable platform for investigating common cellular functions: attachment, viability, proliferation, cellular properties, membrane states, etc. [15]. Fig. 4 illustrates the morphology of mouse fibroblast 3T3 cells cultured on a PCL film and PAOS films. To a first, visual approximation cells grown on the sorbitol-containing polyester films and the PCL control exhibit no morphological differences. This indicates qualitatively comparable biocompatibility between PAOS and PCL.

We chose to quantify cell response by measuring cell density and cell area distributions. Area distributions are considered because cells are complex, living organisms and measured responses may not always follow a normal distribution. As such, reducing the data to a mean and standard deviation may forfeit critical information. Automated fluorescence microscopy was utilized to avoid introducing inadvertent sampling bias [12] (Fig. 5). Also, the automated process for acquiring and analyzing data facilitates larger sampling sizes thereby enhancing the statistical significance of our measurements.

Fig. 6 demonstrates the need for such a rigorous experimental design in that the area distributions appear to vary for the PCL controls. The distributions represent samplings of roughly 200, 300 and 400 cells, respectively. It is difficult to conclude whether all are a subset of the same population from visual comparison alone. To quantify comparisons we employ a nonparametric

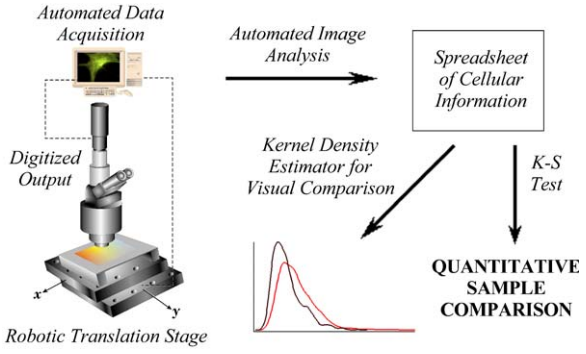

Fig. 5. Scheme for automated sample collecting and sample analysis.

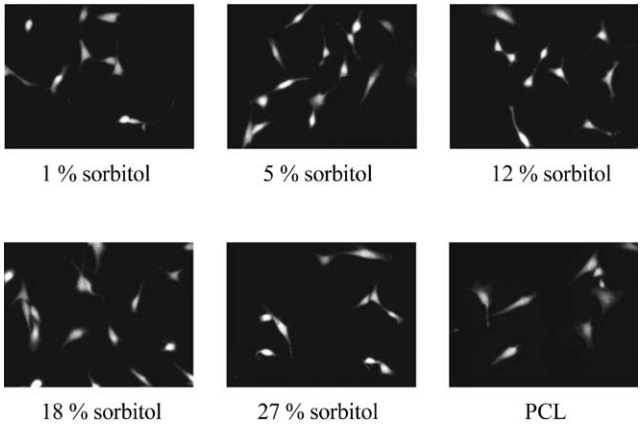

Fig. 4. Fluorescence microscopy images of fibroblast on PCL and PAOS films. Percentages represent the mole fraction of sorbitol.

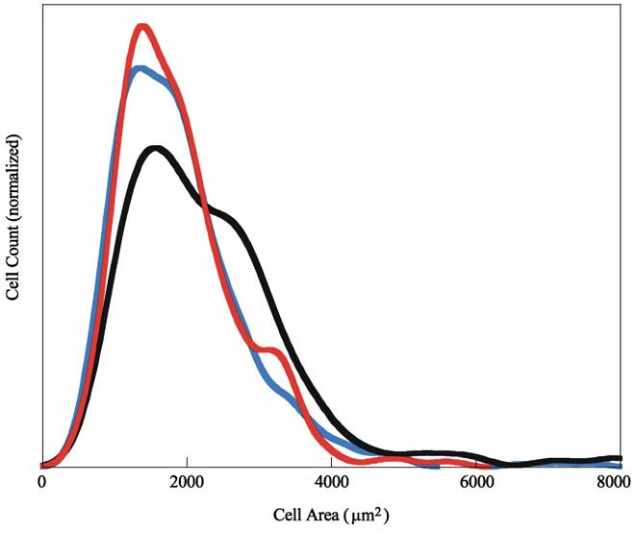

Fig. 6. Cell area distributions for triplicate PCL controls. All data were collected over a continuous run.

Table 2
K–S test results comparing each PAOS against the others as well as the PCL control

	1%	5%	12%	18%	27%	PCL
1%	—	N	N	N	N	N
5%	N	—	N	N	N	N
12%	N	N	—	N	N	N
18%	N	N	N	—	N	N
27%	N	N	N	N	—	95
PCL	N	N	N	N	95	—

Percentages represent the mole fraction of sorbitol.

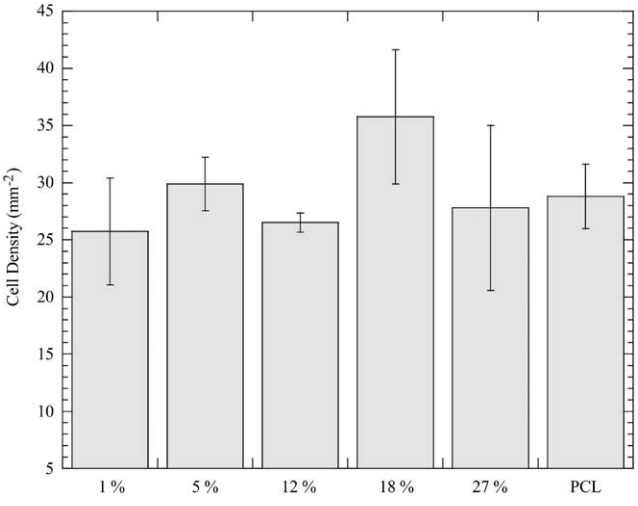

Fig. 7. Cell density on PCL and PAOS films after 24 h culture. Percentages represent the mole fraction of sorbitol.

two-sample (K–S) test [13] that tests the null hypothesis that two samples are randomly selected from the same *general* (i.e. not normal) population against the alternative that the two samples are drawn from different general populations. Our current algorithm reports whether the null hypothesis can be rejected at one of three discreet confidence levels: 90%, 95%, or 99%. Any level less than 90% is regarded as insufficient for rejection. The test reveals that the null hypothesis cannot be rejected when testing any pairs of samples represented by the distributions shown in Fig. 6.

Table 2 summarizes the results of the K–S test where each sorbitol containing polyester is tested against the others as well as the PCL control. A numerical entry indicates the confidence level at which the null hypothesis can be rejected; the letter "N" indicates that the null hypothesis cannot be rejected. Table 2 demonstrates that four of the five sorbitol containing polyesters elicit similar cell spreading to the PCL control and that only the 27% sorbitol sample elicits a response statistically different than PCL. However, the 27% sorbitol sample does elicit a morphological response similar to all other POAS samples. Furthermore, cell counting indicates that all samples elicit a similar proliferative response [16]. The measured cell densities on all materials after 24 h in culture are shown in Fig. 7. All variations fall within the scope of experimental error introduced by the unavoidable variance in seeding density.

As we seek to establish the PAOS polyesters as viable biomaterials, we interpret the whole of our results and conclude that the PAOS copolymers offer similar biocompatibility to PCL. The outlying morphological response of the 27% sorbitol sample will be investigated in greater detail as the functional PAOS backbones are used to develop a platform for more advanced biomaterials. These initial results lay a foundation upon which this platform can be built.

4. Conclusions

In this study, a series of sorbitol-containing polyesters were successfully prepared by lipase-catalyzed condensation polymerization. The polymer films were spin-coated and surface morphology was assessed by AFM. The AFM measurements found a slight decrease in surface roughness attributed to lower crystallinity from 1% to 27% sorbitol content. The water contact angle measurements indicated that PAOS samples with 1% to 27% mol fraction sorbitol units as well as PCL had a similar hydrophobic surface. For cell culture studies that compared the sorbitol-containing polyester and PCL, the cells were shown to spread and proliferate similarly. This investigation indicates that the sorbitol-containing polyesters and PCL have comparable biocompatibility. These results establish the sorbitol-containing polyester series as a promising material for tissue engineering research and development.

References

[1] Griffith LG, Naughton G. Tissue engineering-current challenges and expanding opportunities. Science 2002;295:1009–14.
[2] Temenoff JS, Mikos AG. Review: tissue engineering for regeneration of articular cartilage. Biomaterials 2000;21:431–40.
[3] Hench LL, Polak JM. Third-generation biomedical materials. Science 2002;295:1014–7.
[4] Cook AD, Hrkach JS, Gao NN. Characterization and development of RGD-peptide-modified poly(lactic acid–co-lysine) as an interactive, resorbable biomaterial. J Biomed Mater Res 1997;35:513–23.
[5] Zhu HG, Ji J, Lin RY, Gao CY, Feng LX, Shen JC. Surface engineering of poly(DL-lactic acid) by entrapment of alginate-amino acid derivatives for promotion of chondrogenesis. Biomaterials 2002;23:3141–8.
[6] Quirk RA, Chan WC, Davies MC, Tendler SB, Shakesheff KM. Poly(L-lysine)-GRDDS as a biomimetic surface modifier for poly(lactic acid). Biomaterial 2001;22:865–72.
[7] Dong T, Dubois P, Grandfils C, Jerome R. Ring–opening polymerization of 1,4,8-Trioxaspiro[4.6]-9-undecanone: a new route to aliphatic polyesters bearing functional pendent groups. Macromolecules 1997;30:406–9.

[8] Chen XH, Gross RA. Versatile copolymers from [L]-Lactide and [D]-Xylofuranose. Macromolecules 1999;32:308–14.
[9] Gross RA, Kumar A, Kalra B. Polymer synthesis by in vitro enzyme catalysis. Chem Rev 2001;101:2097–124.
[10] Kumar R, Gross RA. Biocatalytic route to well-defined macromers built around a sugar core. J Am Chem Soc 2002;124:1850–1.
[11] Kumar A, Gross RA. unpublished results.
[12] Elliott JT, Tona A, Woodward JT, Jones PL, Plant AL. Thin films of collagen effect smooth muscle cell morphology. Langmuir 2003;19:1506–14.
[13] Hollander M, Wolfe DA. Nonparametric statistical methods. New York: Wiley, 1973. 503p.
[14] Fu HY, Gross RA. unpublished results.
[15] Trentani L, Pelillo F, Pavesi FC, Ceciliani L, Cetta G, Forlino A. Evaluation of the $TiMo_{12}Zr_6Fe_2$ alloy for orthopeadic implants: in vitro biocompatibility study by using primary human fibroblasts and osteoblasts. Biomaterials 2002;23:2863–9.
[16] Chupa JM, Foster AM, Summer SR, Madihally SV, Matthew HWT. Vascular cell responses to polysaccharide materials: in vitro and in vivo evaluations. Biomaterials 2001;21:2315–22.